Ultraviolet Absorption of Insulators. III. fcc Alkali Halides*

J. C. PHILLIPS†
Department of Physics and Institute for the Study of Metals, University of Chicago, Chicago, Illinois

(Received 12 March 1964; revised manuscript received 20 July 1964)

The optical spectra of the alkali halides are divided into interband scattering and exciton structure. The scattering or direct-transition structure is shown to be similar to that of the zincblende crystals studied in earlier papers of this series. On this basis the band structure $E(k)$ is deduced empirically from the spectra for [100] and [111] axes in k space. The results for the valence bands agree well with Howland's calculations for KCl. The exciton structure is shown to contain extra peaks which overlap the scattering continuum. These are called metastable excitons in contrast to the conventional halogen doublet. It is shown that there is an intimate connection between the scattering and exciton spectra; the latter can only be explained in terms of the former. It is conjectured that the extra excitons are metastable because of self-trapping.

1. INTRODUCTION

THE fundamental absorption spectra of crystals in the ultraviolet were first studied by Hilsch and Pohl.[1] For transmission studies alkali halide films are particularly convenient. Although these spectra have been known for decades, very little quantitative interpretation has been carried out above the fundamental absorption edge. Because of the large effective masses and low dielectric constants the Coulomb interaction between electrons and holes produced by photon absorption is large. Thus in addition to direct interband absorption into independent electron and hole scattering states, a large fraction of the absorption takes place with the production of bound electron-hole pairs (excitons).

The first two narrow absorption peaks are easily identified[1] as "halogen doublets." At higher energies a series of irregularly spaced peaks is encountered. The central problem of interpreting alkali halide electronic spectra is sorting these peaks into those due to excitons and those due to Van Hove singularities in the interband density of states. (The latter account almost completely for the fundamental absorption spectra of diamond and zincblende semiconductors.[2–4]) In the course of preparing a review article[5] on the fundamental absorption spectra of solids, we were led to review the data on alkali halides. It became apparent that because the Brillouin zones of the NaCl and zincblende crystals are those of the fcc sublattices, strong similarities between the energy bands and optical spectra were to be expected. These enable one to disentangle the scattering spectrum from the exciton spectrum, and provide a rather complete analysis of both.

In Sec. 2 we discuss the scattering spectra alone. The exciton peaks can then be sorted out and their fine structure discussed in Sec. 3. In each section we begin by discussing only two crystals in detail, and then extend the analysis to the remaining alkali halides crystallizing in the fcc NaCl structure in Sec. 4.

The experimental data that we have used came principally from two sources. Below 12 eV absorption can be measured with great precision by transmission through thin films mounted on LiF substrates. Eby, Teegarden, and Dutton (ETD)[6] have measured the absorption of a large number of alkali halides in this way at room temperature and at nitrogen temperature, where phonon life-time broadening is much reduced. Above 12 eV absorption from the substrate distorts the film spectra. In the range 10–20 eV we have relied on the reflectance data of Philipp and Ehrenreich,[7] which they have transformed with the aid of the Kramers-Kronig relations. They have taken data at room temperature, with fewer points than in the film work, and only on KCl, KBr, and KI. Their work enables us to survey the ultraviolet absorption spectrum over a much wider energy range, however, and makes an excellent complement to the detailed work of ETD below 12 eV.

2. DIRECT SCATTERING SPECTRA

Only recently has the direct interband threshold $\Gamma_{15} \rightarrow \Gamma_1$ been identified as a shoulder in the absorption spectrum.[8] The shoulders in KBr and KI fall at 7.8 and 6.2 eV, respectively, as shown in Figs. 1 and 2. These shoulders, which fortunately are usually separated from the much stronger exciton structure, provide a firm basis for interpreting interband scattering spectra.

To proceed further we need sketches of the energy bands of the alkali halides. No complete calculations including conduction bands as well as valence bands

* Supported in part by the National Science Foundation and the U. S. Office of Naval Research, and a general grant to the Institute for the Study of Metals by Advanced Research Projects Administration.

† Alfred P. Sloan Fellow.

[1] R. Hilsch and R. W. Pohl, Z. Physik. **59**, 812 (1930).

[2] D. Brust, J. C. Phillips, and F. Bassani, Phys. Rev. Letters **9**, 94 (1962).

[3] D. Brust, M. L. Cohen, and J. C. Phillips, Phys. Rev. Letters **9**, 389 (1962).

[4] J. C. Phillips, Phys. Rev. **133**, A452 (1964), paper II in this series.

[5] J. C. Phillips, Solid State Physics (to be published).

[6] J. E. Eby, K. J. Teegarden, and D. B. Dutton, Phys. Rev. **116**, 1099 (1959).

[7] H. R. Philipp and H. Ehrenreich, Phys. Rev. **131**, 2016 (1963).

[8] E. A. Taft and H. R. Philipp, Phys. Chem. Solids **3**, 1 (1957).

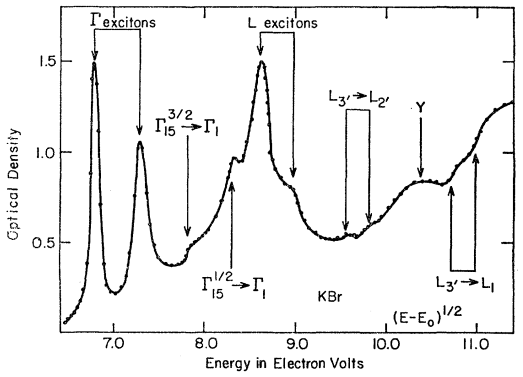

FIG. 1. The absorption spectrum of KBr films at 80°K according to ETD.

are available. Howland[9] has studied the valence bands alone of KCl by the tight-binding method. Rather than rely on his calculations, we adopt a semiempirical approach which regards the valence bands (electrons on the negative ions) as a narrower version of the valence bands of the zincblende crystals. In contrast to the latter, the conduction bands of the alkali halides, which are orthogonal to valence states localized on the anions, are expected to be nearly free-electron over-all. There are two reasons for this:

(1) The effective potential[10,11] of the alkali atoms is very weakly attractive, as proved by the nearly free-electron bands found for alkali metals.

(2) The effective potential of the negative ions for conduction band states is nearly zero (slightly repulsive, on chemical grounds). This is a consequence of the cancellation theorem.[11]

With these ideas in mind we sketch in Fig. 3 the important energy bands for a fcc alkali halide near the energy gap. We place the zero of energy at the top of the spin-orbit split valence band at $k=0$, i.e., set $\Gamma_{15}^{3/2}=0$. The important structure in the valence band is determined by the spin-orbit splitting parameter λ; this can be estimated[6] from the splitting of the free halogen doublet by $3\lambda/2$. It is listed in Table I. Other

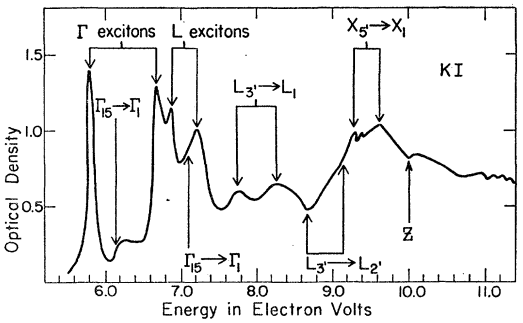

FIG. 2. The absorption spectrum of KI films at 80°K according to ETD.

[9] L. P. Howland, Phys. Rev. **109**, 1927 (1958).
[10] J. C. Phillips, Phys. Chem. Solids **11**, 226 (1959).
[11] M. H. Cohen and V. Heine, Phys. Rev. **122**, 1821 (1961).

TABLE I. Spin-orbit splitting parameters λ for the p valence states of the free halide atoms.

Halide	λ (eV)
F	0.03
Cl	0.07
Br	0.31
I	0.63

important valence band parameters are the width W_L from $\Gamma_{15}^{3/2}$ to the average of the $L_{3'}$ levels and the similar width between $\Gamma_{15}^{3/2}$ and $X_{5'}$.

The situation in the conduction band is more involved. There are two possible models: a nearly free s-p electron model, which would make the conduction

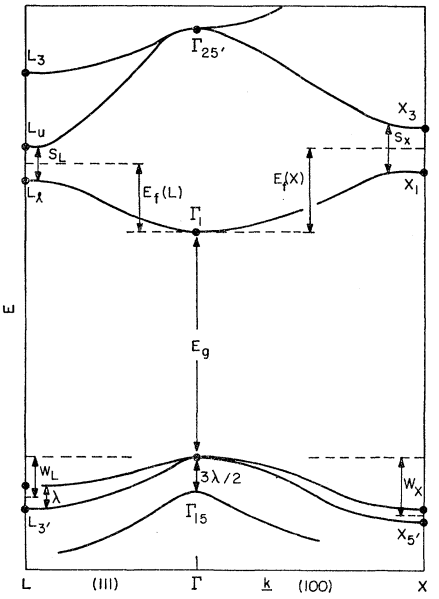

FIG. 3. A schematic band structure for the alkali halides.

band a repetition of the valence band at higher energies; or a modified free-electron model including s-d bands. The d bands centered on the halogen atoms replace the p bands centered on the alkalies. In the absence of a complete band calculation, it is difficult to choose between the models *a priori*. Our schematic model using s-d bands is constructed to resemble the solid rare gases discussed in the following paper.

To determine the scale of energies in the conduction band we introduce the free-electron energies at X and L relative to Γ_1. These are denoted by $E_f(X)$ and $E_f(L)$ and are given by

$$E_f(X)=h^2/2ma^2, \tag{2.1}$$

$$E_f(L)=3h^2/8ma^2, \tag{2.2}$$

where a is the lattice constant. We assume, as usually holds for the nearly free electron model,[12] that the

[12] M. H. Cohen and V. Heine, in *Advances in Physics*, edited by N. F. Mott (Taylor and Francis, Ltd., London, 1958), Vol. 7, 395.

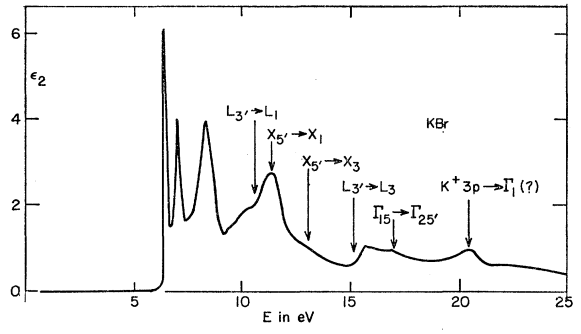

FIG. 4. The imaginary part of the dielectric constant of KBr in the far uv according to Ref. 7.

center of gravity of the two lowest conduction band levels at X is $E_f(X)$, while that of the L_1 and $L_{2'}$ conduction band levels is $E_f(L)$. The splittings of the two lowest conduction band levels at X and L are S_X and S_L, respectively.

We now proceed to determine these parameters for KBr and KI. In both cases λ is large enough to resolve the spin-orbit splitting of $L_{3'}$ and in KI also the splitting of $X_{5'}$.

In the zincblende crystals the strongest reflectance peak[4] was due to $(X_5\rightarrow X_1,X_3)$ which gave Van Hove edges of type M_1, and $\Sigma_4\rightarrow\Sigma_1$, which gave a Van Hove edge of type M_2 and accounted for the peak character. This peak is immediately identifiable in the far-ultraviolet reflectance shown in Fig. 4. The $(X_{5'}\rightarrow X_1$, $\Sigma_4\rightarrow\Sigma_1)$ peak comes at 11.5 eV in KBr, followed by the $X_{5'}\rightarrow X_3$ shoulder which was observed in several III–V crystals by Greenaway.[13] For KI the $X_{5'}\rightarrow X_1$ peaks are at 9.3 and 9.6 eV, while $X_{5'}\rightarrow X_3$ falls at 11.5 eV (see Fig. 5). Apparently the spin-orbit splitting of $X_{5'}$ is about $\lambda/2$. In the diamond lattice the splitting of the analogous level X_4 is zero. From the relations

$$S_X=(X_{5'}\rightarrow X_3)-(X_{5'}\rightarrow X_1)\,, \quad (2.3)$$

$$(X_{5'}\rightarrow X_1)=W_X+E_g+E_f(X)-S_X/2\,, \quad (2.4)$$

we obtain S_X and W_X for KBr and KI, also shown in the table.

The strength of the shoulders assigned to $X_{5'}\rightarrow X_3$ favors X_3 over $X_{4'}$ (the level that would occur in the nearly free-electron model). The transition $X_{5'}\rightarrow X_3$ is allowed while $X_{5'}\rightarrow X_{4'}$ is electric dipole forbidden. The latter possibility cannot be excluded entirely, because the oscillator strength increases linearly as one goes away from X, so that a high density of interband states can still produce the observed peak.

We now turn to transitions between the $L_{3'}$ state and the L_1, $L_{2'}$ states. Here $L_{3'}\rightarrow L_1$ is allowed and $L_{3'}\rightarrow L_{2'}$ is first-order forbidden. Let us denote the lower (upper) of the $(L_1, L_{2'})$ pair by L_l (L_u). With the band structure shown in Fig. 3 the interband density of states for $L_{3'}\rightarrow L_l$ transitions produces a Van Hove singularity of type M_1.

The splitting parameter λ for the level $L_{3'}$ in KI is 0.6 eV. Two M_1 edges can easily be identified at 7.7 and 8.3 eV; these are assigned to $L_{3'}\rightarrow L_l$. The peaks are strong, corresponding to allowed transitions, so that in KI $L_l=L_1$. Very much weaker peaks can be identified in KBr at 9.5 and 9.8 eV. Again the transition is $L_{3'}\rightarrow L_l$, but in KBr $L_l=L_{2'}$ because of the low oscillator strength.

Our next problem is to identify the $L_{3'}\rightarrow L_u$ transitions. According to Fig. 3, these will probably be responsible for the band-4 $\rightarrow$ band-6 threshold (Van Hove singularity of type M_0). If the threshold corresponds to an allowed transition, the absorption coefficient is proportional to $(E-E_0)^{1/2}$. This is seen to be the case for the spin-orbit split thresholds at 10.6 and 10.9 eV in KBr. This means $L_u=L_1$ in KBr, confirming our conclusion that $L_l=L_{2'}$. On the other hand, for a forbidden transition the absorption coefficient is proportional to $(E-E_0)^{3/2}$. This is seen to be the case for the 8.7- and 9.3-eV thresholds in KI, which again show the spin-orbit splitting characteristic of the iodide atom. This means $L_u=L_{2'}$ which confirms our assignment of L_l to L_1 in KI.

With these transitions identified we calculate S_L and W_L from

$$S_L=(L_{3'}\rightarrow L_{2'})-(L_{3'}\rightarrow L_1)\,, \quad (2.5)$$

$$(L_{3'}\rightarrow L_1)=W_L+E_g+E_f(L)-S_L/2\,. \quad (2.6)$$

The values are shown in Table III. Note that the sign of S_L is reversed between KBr and KI.

Before using these results to construct the energy bands of KBr and KI along the principal symmetry directions, we wish to comment on the broad absorption peak marked Y in KBr between 9.9 and 10.6 eV (Fig. 1). It appears that this peak is due to interband transitions, but until a complete analysis of the energy bands throughout the Brillouin zone is made (analogous to those of Refs. 2 and 3), no definite assignment can be made. This same broad peak seems to occur between

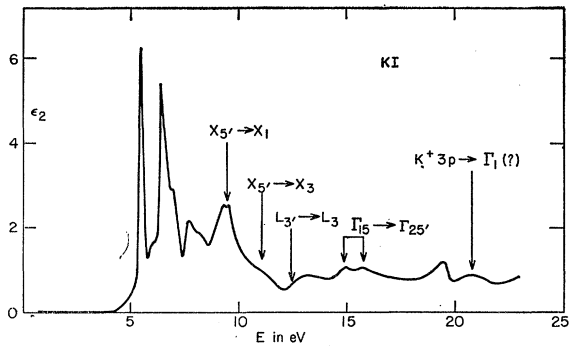

FIG. 5. The imaginary part of the dielectric constant of KI in the far uv according to Ref. 7.

[13] D. L. Greenaway, Phys. Rev. Letters **9**, 97 (1962); D. L. Greenaway and M. Cardona, *Exeter Semiconductor Conference* (Institute of Physics, London, 1962).

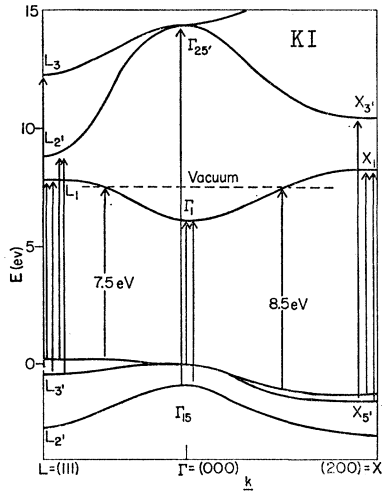

FIG. 6. The energy bands of KI along the [100] and [111] axes, as deduced empirically in Sec. 2.

8.4 and 8.7 eV in KI, distorting the line shape of the upper spin-orbit split $L_{3'} \rightarrow L_1$ doublet.

With the information of Table III, we plot in Fig. 6 the energy bands of KI along the [100] and [111] symmetry axes; a similar sketch for KBr is given in Fig. 7. Note that for both crystals the top of the valence band is probably $L_{3'}$. One would expect weak indirect absorption thresholds for both crystals about 0.3 eV below the direct absorption threshold. If these are present they are obscured by the first exciton peak.

In the rare-gas atoms, which are isoelectronic to halide ions, the transitions $np^6 \rightarrow np^5nd$ occur at slightly higher energies than $np^6 \rightarrow np^5(n+1)s$. Transitions to the d states $\Gamma_{25'}$ and L_3 in the conduction band may be identifiable in the alkali halides. By comparison with solid argon (following paper) we expect allowed transitions $p \rightarrow d$ to fall near 14 eV in KI and near 16 eV in KBr. We see that there are further absorption peaks in this region, and that the KBr peaks are each about 2 eV higher than the analogous peaks in KI. Because the KI peak at 15 eV seems to show a spin-orbit splitting of 0.9 eV, we have assigned it to $\Gamma_{15} \rightarrow \Gamma_{25'}$ and the lower peak to $L_{3'} \rightarrow L_3$.

At higher energies we enter the soft x-ray region where absorption begins first from the K^+ $3p$ core levels (at about 20 eV according to free atom term values) and then from Cl^- $3s$ core levels (at about 25 eV, according to Howland[9]). (We assume that there is no Madelung correction to the free-atom excitation energies, as would be the case if the excited electron were localized on the same atom as the core hole.) It is possible that the peak at 21 eV in KCl, KBr, and KI is caused by $K^+3p \rightarrow (\Gamma_1)$ conduction band transitions. This point could be clarified by studying the Rb salts, where the free atom transition from the $4p$ core level requires 16 eV or the Cs salts ($5p$ core level, 13 eV).

The foregoing discussion is easily extended to include KCl. The results are shown in Tables II and III and the energy bands in Fig. 8 (Howland's band calculations

TABLE II. Interband transitions in KBr, KI, and KCl in eV.

Interband transition	KBr	KI	KCl
$\Gamma_{15}(\frac{3}{2}) \rightarrow \Gamma_1$	7.8	6.1	8.5
$\Gamma_{15}(\frac{1}{2}) \rightarrow \Gamma_1$	8.3	7.0	···
$L_{3'}(\frac{3}{2}) \rightarrow L_1$	10.7	7.25	···
$L_{3'}(\frac{1}{2}) \rightarrow L_1$	11.0	7.75	···
$L_{3'}(\frac{3}{2}) \rightarrow L_{2'}$	9.5	8.45	10.35
$L_{3'}(\frac{1}{2}) \rightarrow L_{2'}$	9.8	8.90	10.45
$L_{3'} \rightarrow L_3$	15.2	12.2	16
$X_{5'} \rightarrow X_1$	11.5	9.3,9.6	12.6
$X_{5'} \rightarrow X_3$	13.3	11.5	13.7
$\Gamma_{15}(\frac{3}{2}) \rightarrow \Gamma_{25'}$	17.0	14.3	···
$\Gamma_{15}(\frac{1}{2}) \rightarrow \Gamma_{25'}$	···	15.2	···
$[Y]$	[9.9,10.7]	[8.4,8.7]	···

TABLE III. The values in eV of the band parameters of Fig. 3 inferred from the data of Table II and equations (2.1) and (2.2) of the text.

Parameter	KBr	KI	KCl
$E_f(X)$	3.5	3.0	3.9
$E_f(L)$	2.6	2.3	2.9
W_X	1.1	1.4	0.7
W_L	−0.2	0.1	···
S_X	1.8	2.0	1.2
S_L	−1.2	1.0	···

qualitatively confirm the position of $L_{3'}$ in the valence bands of KBr and KI. Therefore his calculations can be used to place $L_{3'}$ in KCl.) Note that in this case the spin-orbit splittings are too small to be resolved except in the halogen doublet exciton peaks (Sec. 3).

Our analysis also can be extended to the other fcc alkali halides in the region below 10 eV where data is available (Sec. 4). Before doing this, we analyze the exciton spectra of the iodides.

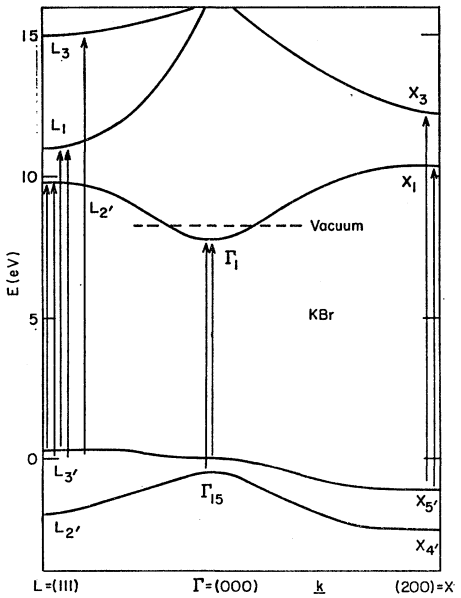

FIG. 7. The energy bands of KBr along the [100] and [111] axes, as deduced empirically in Sec. 2.

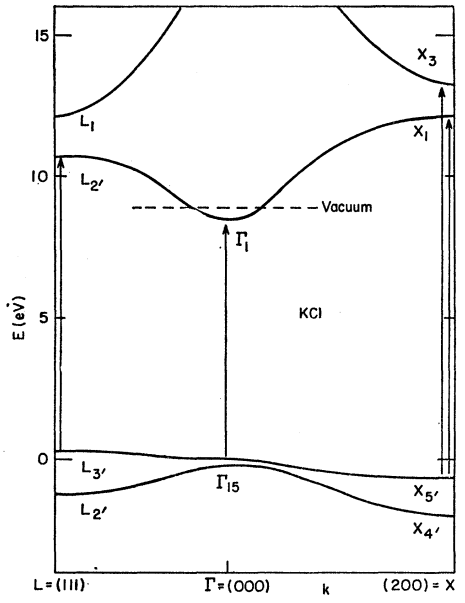

FIG. 8. The energy bands of KCl.

3. INTERBAND EXCITON SPECTRA

The first attempts to interpret the structure of the exciton spectra in alkali halide crystals were made by Hilsch and Pohl[1] and by Mott,[14] who pointed out that most of the spectra of the iodides and bromides exhibit a strong doublet structure, at least in the first absorption peak. The separation of this doublet is about $3\lambda/2$, the separation of the ground-state doublet of the free halogen atom. Photoemission studies[8] have shown that free electrons are not produced when one or both of the narrow absorption peaks lies below the threshold defined by Philipp and Taft for interband scattering spectra.

Theoretical attempts to interpret exciton spectra were based for many years on atomic-orbital models similar to those used in crystal-field theory.[15–17] These readily provide an explanation for the first exciton doublet, but they encounter very serious problems in treating the remaining exciton peaks. In the KI spectrum shown in Fig. 2, the first doublet at 5.80 and 6.68 eV is split by 0.88 eV, as expected from the iodide splitting $3\lambda/2=0.9$ eV. This doublet, however, is followed by two more exciton peaks at 6.90 and 7.30 eV. Additional peaks are also obvious in the other iodides. Our analysis will show that extra exciton peaks are in fact present in most of the spectra.

Overhauser[16] and also Knox and Inchauspe[17] have attempted to explain these extra peaks in terms of an atomic-orbital model. The first two peaks correspond to wave functions formed from linear combinations of a p hole on the halide and an s electron on the alkali. The extra peaks are due to linear combinations of p halide holes and d halide electrons chosen to transform as vectors (electric dipole coupling of the ground state of the crystal to the exciton state).

There are several reasons for suspecting this model. Empirically it has not led to the positive identification of any of the extra exciton peaks. From a theoretical viewpoint it is even more deeply dubious. As stressed in the energy-band model of the preceding section, the conduction-band states are much more nearly those of free electrons than atomic orbitals. Indeed, if one looks for d-like states such as $\Gamma_{25'}$ at $k=0$ in the conduction band one finds them about 15 eV or more above the top of the valence band. Such states are energetically excluded from contributing the extra exciton peaks.

The deepest reason for suspecting atomic orbital models has emerged in our review of the fundamental absorption spectra of crystals. We have repeatedly found in many crystals an intimate connection between the interband scattering spectra and exciton spectra. (In semiconductors where excitons are weakly bound, their effect is chiefly to sharpen interband scattering edges.) Now it is known that the great weakness of the atomic orbital or tight binding model is that the atomic orbitals do not form a complete set because of the omission of continuum (scattering) states. A more general band model of exciton states is therefore required.

Such a model was first provided by Slater and Shockley.[18] It has been the subject of a number of theoretical papers. All work on alkali halides has so far considered only excitons associated with the first fundamental absorption edge (of type M_0). There is now abundant experimental evidence in zincblende crystals that excitons are also formed at M_1 (saddle-point or hyperbolic) edges. We propose to explain the extra exciton peaks in terms of these metastable or "dynamically unstable excitons" which in our case overlap the electron-hole scattering continuum.

The model interband density of states we have in mind is shown in Fig. 9 (no spin-orbit splitting). An M_0 edge derived from interband transitions at Γ occurs at E_0. Associated with it is the conventional exciton at E_0-B_Γ, where B_Γ is the binding energy. Similarly an M_1 Van Hove edge derived from interband transitions at L is located at E_1. Associated with it is a dynamically unstable exciton at E_1-B_L, where B_L is the binding energy of the metastable L exciton.

At first sight one may feel that metastable excitons are an artificial construct which cannot be either proved or disproved. For example, calculation of B_Γ has proved difficult for excitons in alkali halides. (The binding is so strong that one cannot make the effective mass approximation, and the exciton radius is so small that

[14] N. F. Mott, Proc. Roy. Soc. (London) **A167**, 384 (1938).
[15] D. L. Dexter, Phys. Rev. **108**, 707 (1957).
[16] A. W. Overhauser, Phys. Rev. **101**, 1702 (1956).
[17] R. S. Knox and N. Inchauspe, Phys. Rev. **116**, 1093 (1959).
[18] J. C. Slater and W. Shockley, Phys. Rev. **80**, 705 (1936).

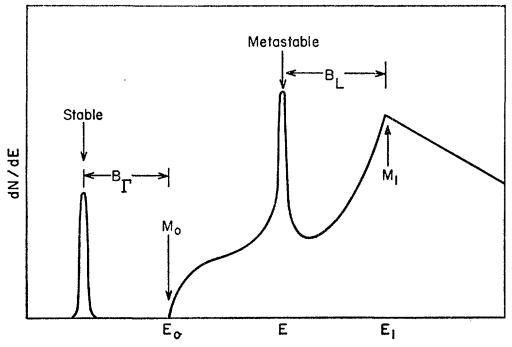

FIG. 9. Schematic model for stable and metastable excitons (no spin-orbit splitting).

the short-range screening of the electron-hole Coulomb interaction is not given by the static dielectric constant.) We will not even attempt to calculate B_L, because of the hyperbolic interband energy surfaces involved.

Nevertheless there are a number of empirical clues that will prove our conjecture. These are similar to the ones used for identifying interband scattering spectra. The most important one is the spin-orbit splitting. Just as the spin-orbit splitting of the Γ exciton is determined by the splitting of Γ_{15}, so the splitting of the metastable L exciton is determined by that of $L_{3'}$. Some care is necessary here. Because of the presence of 4 neighborhoods of L broadening effects arise. These tend to spread out the wave packets sway from Λ, the (111) symmetry axis of orbital degeneracy where the spin-orbit splitting is λ. The greater B_L, the large the spread in k space. This has the effect of reducing the spin-orbit splitting below the value λ.

To illustrate our method of analysis we discuss KI and RbI in detail. As shown in Fig. 2 and Fig. 10 there are four important exciton peaks. The energies are shown in Table IV.

Consider first the Γ exciton. The binding energy of the $J=\frac{3}{2}$ exciton is computed from

$$B_\Gamma(\tfrac{3}{2})=E(\Gamma_1-\Gamma_{15}{}^{\frac{3}{2}})-\epsilon(\Gamma_{\frac{3}{2}}), \qquad (3.1)$$

where ϵ is the exciton energy. The binding energy is 0.4 eV in both KI and RbI. The $\Gamma_{15}{}^{\frac{1}{2}}\rightarrow\Gamma_1$ threshold in RbI is a well defined shoulder at 6.75 eV. The shoulder is probably also well defined in KI, but has probably not been observed because of the sparsity of experimental

TABLE IV. Stable and metastable excitons in the iodides.

	$J(m_J)$	KI	RbI	NaI
ϵ_Γ	$\frac{3}{2}$	5.80	5.70	5.56
	$\frac{1}{2}$	6.68	6.47	6.73
λ_Γ		0.88	0.77	1.17
B_Γ	$\frac{3}{2}$	0.4	0.4	0.25
	$\frac{1}{2}$	0.3	0.3	0.20
ϵ_L	$\frac{3}{2}$	6.88	6.65	7.35
	$\frac{1}{2}$	7.25	6.95	8.0
λ_L		0.37	0.30	0.65
B_L		0.9	0.7	1.1

points between 7.0 and 7.2 eV. By analogy with RbI [and also from the asymmetric line shape of the $(L\,\frac{1}{2})$ exciton] we can place the $\Gamma_{15}{}^{1/2}\rightarrow\Gamma_1$ shoulder in KI at 7.0 eV. This gives $B_\Gamma(\frac{1}{2})$ the value 0.3 eV in both crystals.

The difference between $B_\Gamma(\frac{3}{2})$ and $B_\Gamma(\frac{1}{2})$ provides an excellent qualitative check on our analysis. It is well known that the hole effective mass for the $J=\frac{1}{2}$ state is much smaller than for the $J=\frac{3}{2}$. This reduces the binding energy from 0.4 to 0.3 eV. [If we use a hydrogenic model and assume $m_e=m_h(\frac{1}{2})$ with $m_h(\frac{3}{2})\gg m_e$, then μ, the reduced exciton mass is twice as large for $J=\frac{3}{2}$ as for $J=\frac{1}{2}$ and one would expect $B_\Gamma(\frac{3}{2})=2B_\Gamma(\frac{1}{2})$. This argument is naive, however, as it neglects nonparabolic band effects on the $J=\frac{1}{2}$ exciton compared to $J=\frac{3}{2}$. This factor tends to reduce the binding-energy ratio to the observed value of 1.3.]

The spin-orbit splitting of the Γ excitons is about 0.9 eV. [It is likely that the splitting in RbI is 0.1 eV too small because of subtraction effects due to the Rb^+ splitting. Similar effects, sometimes even giving inverted levels, have been found in cuprous halides.[19]] This is just $3\lambda/2$. For L excitons the expected splitting is $\lambda=0.6$ eV in the iodides. Instead a splitting of 0.4 eV $=2\lambda/3$ is found. We believe this reduction is due to the spreading of wave packets away from L as mentioned above.

The larger volume of momentum space occupied by L excitons is reflected in the binding energy B_L of 0.9 eV, more than twice B_Γ. The enhanced binding energy reflects the flatness of the energy bands near L compared to Γ.

We now turn to a challenging case—NaI (see Fig. 11). Here the Na^+ potential seems to be so weak that the valence electrons are strongly localized on the halide ion, thus increasing the value of $3\lambda/2$ from 0.9 to 1.2 eV. We are not able to specify the details of this enhanced splitting, but we can show that it is maintained not only in the higher exciton peaks but also in the interband spectra. (Thus the enhanced splitting cannot be ascribed to spin-spin interaction in the bound exciton state.) The important exciton energies are also shown

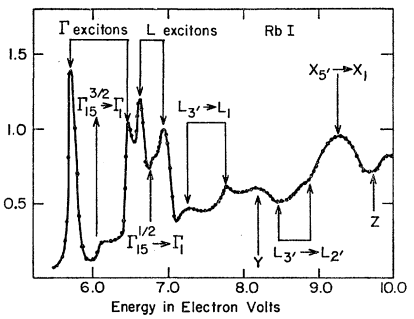

FIG. 10. The absorption spectrum of RbI films at 80°K according to ETD.

[19] M. Cardona, Phys. Rev. **129**, 69 (1963).

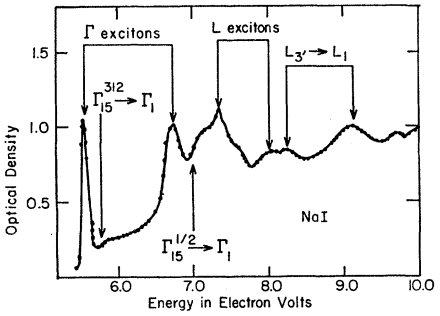

FIG. 11. The absorption spectrum of NaI films at 80°K according to ETD.

in Table IV. It is seen that they follow the same general pattern as KI and RbI, but with the value of λ increased by $\frac{1}{3}$.

In KI and RbI the binding energy B_L is about twice that of B_Γ. In NaI, on the other hand, $B_L \sim 4B_\Gamma$, which suggests that the L binding energy may be affected by the same mechanism that enhances λ in NaI.

4. fcc SCATTERING AND EXCITON SPECTRA

We wish to extend our analysis to other fcc crystals. Many of the spectra are not suited to detailed analysis, however, and we exclude them for the reasons quoted:

(1) The energy gap in the fluorides is of order 10 eV so that too little data are available.

(2) Somewhat more data are available for the chlorides (especially KCl). The latter was discussed partially in Sec. 2. The smallness of the spin-orbit splitting at L (0.08 eV) makes progress on the chlorides difficult. We include some results on NaCl, KCl, and RbCl in Table V. The data ETD attempted to obtain for CsCl in the fcc structure clearly contains a substantial bcc contribution, so we exclude it. Note that the L exciton is present in KCl and RbCl but absent from NaCl. The special case of LiCl is discussed at the end of this section.

(3) For the bromides the situation improves slightly, but KBr is still the best example. The spectrum of RbBr should show as much structure as KBr, but it does not; perhaps the samples were at fault. A summary of our results for the bromides is given in Table VI. Note again that the L exciton is present in KBr and RbBr, but absent in NaBr and LiBr.

TABLE V. Low-energy interband edges and excitons in the chlorides.

	NaCl	KCl	RbCl
	Interband		
$\Gamma_{15}(\frac{3}{2}) \rightarrow \Gamma_1$	8.4	8.5	8.1
$L_{3'} \rightarrow L_{2'}$	10.3	10.35,10.45	9.9
	Excitons		
ϵ_Γ	7.96	7.76	7.51
	8.09	7.87	7.64
ϵ_L	absent	9.5	8.9

TABLE VI. Low-energy interband edges and excitons in the bromides.

	LiBr	NaBr	KBr	RbBr
$\Gamma_{15}^{\frac{3}{2}} \rightarrow \Gamma_1$	7.95	7.5	7.8	7.65
$\Gamma_{15}^{\frac{1}{2}} \rightarrow \Gamma_1$	8.40	7.9	8.3	...
$L_{3'} \rightarrow L_1$	...	...	10.7,11.0	9.4,9.7
$L_{3'} \rightarrow L_{2'}$	...	...	9.5,9.8	8.55,8.85
$\epsilon_\Gamma(\frac{3}{2})$	7.20	6.68	6.77	6.60
$\epsilon_\Gamma(\frac{1}{2})$	7.72	7.20	7.26	7.08
$\epsilon_L(\frac{3}{2})$	absent	absent	8.6	7.85
$\epsilon_L(\frac{1}{2})$	absent	absent	8.9	8.15

A rather fascinating change in electronic character seems to take place as we pass from KBr to NaBr to LiBr. We have interpreted the spectrum of KBr exhaustively and shown that the line shapes conform to conventional expectations. At first sight NaBr merely seems to be a strongly broadened version of KBr. When we examine the LiBr spectrum, however, we realize that NaBr was something similar to a mixed phase.

The first surprising feature of the LiBr spectrum, compared to the crystals discussed above, is the appearance of the interband thresholds as plateaus rather than shoulders (Fig. 12). It would be interesting to have photoemission data to check our interpretation of these thresholds. One should remember[2] that the intrinsic line shape is contained not in the absorption coefficient k, but in $\epsilon_2 = 2nk$. The change in line shape may reflect the variation of n in this region as well as the overlap of the thresholds with the $\Gamma(\frac{1}{2})$ exciton peak.

Compared to the preceding crystals, more surprising still are the almost ideal Van Hove edges V at 9.3 and 10.65 eV. These are much sharper than the M_1 edges at 7.7 and 8.3 eV in KI. Moreover, no spin-orbit splitting is observed. There is structure nearby at 9.8 and 11.05 eV, but it does not have the expected spacing (0.3 eV). Also both peaks are strong, whereas $L_{3'} \rightarrow L_1, L_{2'}$ gives one strong and one weak peak. This may mean that the important edges no longer occur at L, but somewhere else in the Brillouin zone.

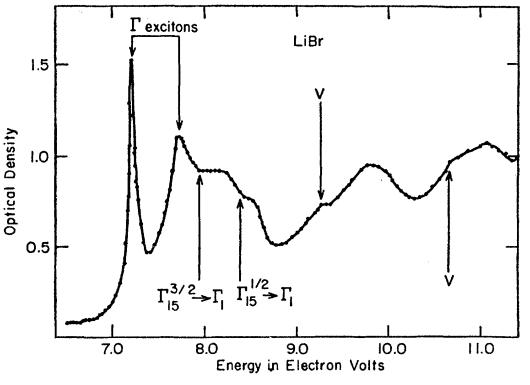

FIG. 12. The absorption spectrum of LiBr films at 80°K according to ETD.

TABLE VII. Low-energy interband edges and excitons in the iodides.

	NaI	KI	RbI
$\Gamma_{15}^{3/2} \rightarrow \Gamma_1$	6.75	6.1	6.0
$\Gamma_{15}^{1/2} \rightarrow \Gamma_1$	7.0	7.0	6.75
$L_{3'} \rightarrow L_1$	8.25,9.15	7.7,8.3	7.25,7.75
$L_{3'} \rightarrow L_{2'}$	...	8.7,9.3	8.45,8.90
$X_{5'} \rightarrow X_1$		9.3,9.6	9.3
Y	...	8.5	8.3
$\epsilon_\Gamma(\frac{3}{2})$	5.56	5.80	5.70
$\epsilon_\Gamma(\frac{1}{2})$	6.73	6.68	6.47
$\epsilon_L(\frac{3}{2})$	7.35	6.88	6.65
$\epsilon_L(\frac{1}{2})$	8.00	7.25	6.95

Note that these changes correlate with the absence of L excitons.

(4) Among the iodides we reject LiI because ETD have been unable to identify the first exciton peak. Structure for NaI, KI, and RbI is shown in Table VII. Note that L_1 is lower than $L_{2'}$ for all three iodides, whereas in KBr and RbBr the opposite was true. This suggests that even in the conduction band the splittings are determined primarily by the halide ion. That s states are lower than p states for heavier atoms is a consequence of s-d hybridization and relativistic effects which are well known for alkalies[20] and semiconductors.[21]

We append here a discussion of the peculiar spectrum of LiCl shown in Fig. 13. The puzzling features of this spectrum are the interband thresholds at 8.48, 8.62 eV which *precede* the exciton doublet at 8.80, 8.92 eV. The interband thresholds exhibit an unusual line shape which may be characteristic of forbidden transitions. We identify them with $L_{3'} \rightarrow L_{2'}$ and suggest that the excitons are primarily L excitons. Their dominant parent interband edge may be the $L_{3'} \rightarrow L_1$ threshold at 9.1 eV, although this assignment is uncertain. They lie above $L_{3'} \rightarrow L_{2'}$ because the latter is forbidden.

5. PHOTOEMISSION

The reflectance data of Philipp and Ehrenreich are accompanied by an extended theoretical commentary.[7]

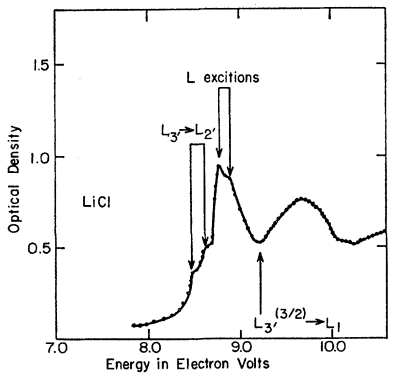

FIG. 13. The absorption spectrum of LiCl films at 80°K according to ETD.

The discussion revolves around exciton states (labeled α) which are analogous to the metastable (or dynamically unstable) excitons conjectured by Cardona and Harbeke[22] and us for semiconductors.[23] None of these exciton states α are explicitly identified in the spectra, but it is finally suggested that *all* the peaks (narrow or broad) are due to excitons. As we have stressed in the introduction, this "universal exciton" hypothesis begs the crucial question of separating bound electron-hole states (excitons) from scattering states.

According to the theoretical commentary,[7] the evidence for the "universal exciton" hypothesis is the lack of structure in the photoemissive yield above threshold, which is in marked contrast with the optical absorption over the same energy range. It is pointed out that there is structure in the photoemissive yield of Si which correlates well with the optical structure.

We have previously given a successful *quantitative* treatment of this problem based on a complete study of the energy bands of Si.[3] The structure in the photoemissive yield of Si can be explained quite simply. The vacuum level lies well above the bottom of the conduction band at X_1. At low photo energies (near 3.5 eV) electrons are excited from the *top* of the valence band to the neighborhood of Γ_{15}, which is *above* vacuum level for a cesiated surface (high yield). At higher photon energies near 4.5 eV the dominant transitions take place from deep valence states near X_4 to the neighborhood of X_1, *below* vacuum level; this causes the yield to drop. Later, near 5.5 eV, the $L_{3'} \rightarrow L_3$ transitions dominate and the yield rises again because L_3 is above vacuum level.

Now consider the specific example of KI, which is supposed[7] to furnish the proof of the "universal exciton" hypothesis. The photoemissive yield rises steeply near 7.5 eV, which enables us to place the vacuum level as shown in Fig. 6. It is immediately obvious from the form of the bands shown there that the direct threshold varies from 7.5 eV along the [111] axis to 8.5 eV along the [100] axis. Apart from spreading the threshold over a range of 1 eV, the band structure should cause no further variation in the yield above 8.5 eV. The observed plateau in the photoemissive yield merely provides a lower limit on the position of L_1. It in no way contradicts the identification of interband scattering Van Hove edges.

We conclude with some comments on the photoelectron energy distribution for KCl (Fig. 14) reported by Taylor and Hartman.[24] Their results show the greatest structure for $\hbar\omega = 13.8$ eV. Two superimposed peaks can be resolved in dN/dE, centered at 1.5 and 3 eV. We believe (see Fig. 8) that the former electrons come from the neighborhood of $L_{2'}$, the latter from the neighborhoods of X_1 and L_1.

[20] F. S. Ham, Phys. Rev. **128**, 2524 (1962).
[21] J. C. Phillips, Phys. Rev. **125**, 1931 (1962).
[22] M. Cardona and G. Harbeke, Phys. Rev. Letters **8**, 90 (1962).
[23] J. C. Phillips, Phys. Rev. Letters **10**, 329 (1963).
[24] J. W. Taylor and P. L. Hartman, Phys. Rev. **113**, 1421 (1959).

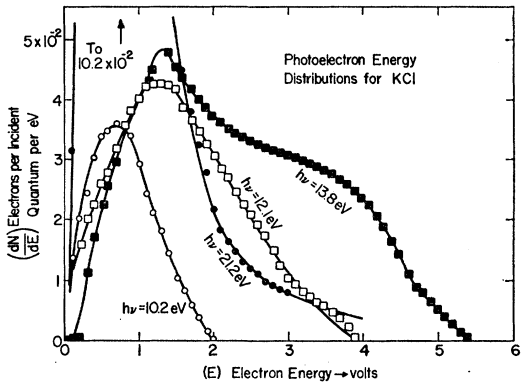

FIG. 14. Photoelectron energy distributions in KCl, with photon energy as a parameter (Taylor and Hartman, Ref. 24).

6. CONCLUSIONS

So much data has been surveyed that it is well to take stock at this point and analyze the significance of the results.

With regard to the interband spectra a number of important edges at Γ, X, and L have been identified. Because of the nearly free-electron character of the conduction band, these account for most of the interband edges. (Cf. Ge[2], where the lowest conduction band has an extra oscillation along Λ, which introduces extra edges.) Not all of the interband structure has been identified: in KI and RbI the interband peak Y and threshold Z are well defined, but probably come from some part of the Brillouin zone such as the [110] axis or the corners W. Such structure is better treated within the framework of an interpolation scheme similar to that successfully applied to semiconductors.[2,3]

The schematic band model that we have introduced in Sec. 2 depends essentially on the assumption that (2.1) and (2.2) give the center of gravity of the two lowest conduction bands at X and L. From this assumption one concludes that at least in KBr and KI the top of the valence band is at L, not, as usually holds, at Γ. If we try to shift $L_{3'}$, L_1, and $L_{2'}$ down in energy so that $L_{3'}$ is no longer the top of the valence band, then L_1 falls below the vacuum level, and a dip in the photoemission would be observed near 8.3 eV. This provides circumstantial support for our simplified band model.

In KCl, KBr, and KI, as well as RbI, our model places the center of gravity of $L_{3'}$ about 0.3 eV above the center of gravity of Γ_{15}; Howland's tight-binding calculation[9] of the valence bands of KCl also places $L_{3'}$ 0.3 eV above Γ_{15}. He claims that the maximum of the valence band is near the (110) zone edge (point K). It is possible, as mentioned above, that interband edges occur near K, but we have not identified them.

Our discussion of the extra excitons (those not associated with the band edge at Γ) can also be divided into phenomenology and a conceptual model. In Secs. 3 and 4 we discussed the former, and established that the extra excitons show a spin-orbit splitting characteristic of the neighborhood of L. The extra excitons might be badly broadened by autoionization, because they overlap the electron-hole scattering continuum near Γ. Their line width is generally comparable to that of the stable excitons.

How can we understand the metastable character of the extra excitons? It cannot be due merely to different regions of k space, for the electron and hole can scatter to the neighborhood of Γ by emitting or absorbing optical phonons. Our only empirical clue is the occurrence of metastable excitons in NaI, KI, RbI, KBr, RbBr, KCl and their absence in LiBr, NaBr, NaCl. In the latter crystals the halogen-halogen overlap is enhanced by the smallness of the metal ion. This suggests the following picture.

The long lifetime of the extra excitons is due to self-trapping. Self-trapping of free holes has been established for several alkali halide crystals by Castner and Känzig.[25] They showed that the hole causes a Jahn-Teller distortion of the lattice which results in the formation of $(\text{halogen})_2^-$ molecules. Of course, because the exciton is neutral, the self-trapping energy in the ionic lattice is much smaller than that of a free hole. Although the free hole in thermal equilibrium seems to be self-trapped, the situation is marginal for autoionization and trapping of the free hole may not occur so rapidly in LiBr, NaBr, or NaCl. For these crystals autoionization would take place more readily, and the extra excitons would tend to "dissolve" into the interband background.

This explanation fits all the crystals except NaI, where the halogen overlap is even larger than in NaCl. Note, however, that in the iodides the spin-orbit splitting is large, which tends to flatten the valence bands (reduce the hole mobility).

Further comments on metastable excitons are contained in the following paper on the simpler system of solid rare gases.

ACKNOWLEDGMENTS

It is a pleasure to thank H. Philipp for copies of his original data, and S. A. Rice and M. H. Cohen for discussions of self-trapping.

[25] T. G. Castner and W. Känzig, Phys. Chem. Solids 3, 178 (1957).